

Studies of the Optics of Neutrons. I. Measurement of the Neutron-Proton Coherent Scattering Amplitude by Mirror Reflection*

W. C. DICKINSON, L. PASSELL,[†] AND O. HALPERN[‡]
Lawrence Radiation Laboratory, University of California, Livermore, California

(Received December 4, 1961)

Measurements were made of the ratio, $a_C/|a_H|$, of the carbon to the hydrogen coherent scattering amplitudes, using liquid hydrocarbon mirrors with various ratios of hydrogen to carbon atoms. In two of these measurements the reflected neutron intensity from different liquids was compared for a fixed angle of reflection. In two other measurements the angles were determined for which the same reflected intensity was obtained.

Our most accurate value for the ratio of the nuclear amplitudes, after various corrections, is $(a_C/|a_H|)$ (nuclear) = 1.775 ± 0.004 . Combining this value with the presently accepted value of the carbon nuclear scattering amplitude, $a_C = (6.64 \pm 0.02) \times 10^{-13}$ cm, we find the best value for the proton scattering amplitude is $a_H = (-3.74 \pm 0.02) \times 10^{-13}$ cm.

I. INTRODUCTION

THE neutron-proton coherent scattering amplitude is an important parameter in the study of nuclear forces and has been measured by a number of different techniques in recent years. Teller¹ was the first to point out that measurement of the neutron scattering by hydrogen should lead to information concerning spin-dependent forces. The first experiments, which involved the comparison of the slow neutron cross sections of ortho- and para-hydrogen,²⁻⁶ proved that the n - p force was spin dependent but did not yield a very precise value for the scattering amplitude because the parahydrogen cross section, from which the scattering amplitude is derived, is small compared to the orthohydrogen cross section. As a consequence the measurement is very sensitive to the presence of small amounts of orthohydrogen impurity. The best value obtained in these experiments was⁶ $a_H = (-3.95 \pm 0.12) \times 10^{-13}$ cm.

Later Shull *et al.* analyzed the Bragg scattering of neutrons by hydrogen in crystals^{7,8} and obtained the value $a_H = (-4.1 \pm 0.2) \times 10^{-13}$ cm. They were not able to improve on the precision of the earlier experiments, however, because of the background from thermal diffuse and spin incoherent scattering of hydrogen and the lack of a satisfactory theory of inelastic neutron scattering. Both results lead to values of the n - n force which were different from the value of the n - p force

obtained in the neutron-proton scattering experiments.⁹

More recently, Burgy, Ringo, and Hughes^{10,11} studied the reflection of neutrons from hydrogen-containing liquids and determined the n - p scattering amplitude in terms of the accurately known carbon scattering amplitude. Their result was of greater precision [$a_H = (-3.78 \pm 0.02) \times 10^{-13}$ cm] than the earlier measurements and in better agreement with the concept of charge independence of nuclear forces. Stewart and Squires¹² then repeated the ortho-, para-hydrogen experiment, taking particular care with the determination of the ortho-para composition of their hydrogen gas, and their result [$a_H = (-3.80 \pm 0.05) \times 10^{-13}$ cm] was in essential agreement with the mirror reflection value.

It has been pointed out by Halpern,¹³ however, that absorption and incoherent scattering processes affect neutron reflection and that the large incoherent scattering cross section of hydrogen might have influenced the mirror reflection experiments to some extent. In view of the importance attached to the understanding of the n - p interaction, it was therefore decided to make a completely independent determination of the scattering amplitude using the mirror reflection method.

II. THE MIRROR REFLECTION METHOD

When a neutron of wave number $k (=mv/\hbar)$ is incident on a reflecting surface at a grazing angle ϕ , the probability that the neutron will be reflected is¹³

$$r(k, a, \phi, \gamma) = \frac{|\phi - (\phi^2 - 4\pi N a / k^2 + i\gamma/k)^{1/2}|^2}{|\phi + (\phi^2 - 4\pi N a / k^2 + i\gamma/k)^{1/2}|^2}, \quad (1)$$

where N is the number of scattering centers per unit volume with bound-atom scattering amplitude a , and $\gamma = N_a \sigma_a + N_i \sigma_i$, where N_a and N_i are the number

* This work was done under the auspices of the U. S. Atomic Energy Commission.

[†] Present address: Atomic Energy Commission, Research Establishment Risø, Roskilde, Denmark.

[‡] Consultant, under contract with the U. S. Atomic Energy Commission.

¹ E. Teller, Phys. Rev. **49**, 420 (1936).

² J. Halpern, I. Estermann, O. C. Simpson, and O. Stern, Phys. Rev. **52**, 142 (1937).

³ F. G. Brickwedde, J. R. Dunning, H. J. Hoge, and J. H. Manley, Phys. Rev. **54**, 266 (1938).

⁴ L. W. Alvarez and K. S. Pitzer, Phys. Rev. **58**, 1003 (1940).

⁵ J. Schwinger, Phys. Rev. **58**, 1004 (1940).

⁶ R. B. Sutton, T. Hall, E. E. Anderson, H. S. Bridge, J. W. DeWire, L. S. Lavatelli, E. A. Long, T. Snyder, and R. W. Williams, Phys. Rev. **72**, 1147 (1947).

⁷ C. G. Shull, E. O. Wollan, G. A. Morton, and W. L. Davidson, Phys. Rev. **73**, 842 (1948).

⁸ C. G. Shull and E. O. Wollan, Phys. Rev. **81**, 527 (1951).

⁹ J. M. Blatt, Phys. Rev. **74**, 92 (1948); J. M. Blatt and J. D. Jackson, Phys. Rev. **76**, 18 (1949).

¹⁰ D. J. Hughes, M. T. Burgy, and G. R. Ringo, Phys. Rev. **77**, 291 (1950).

¹¹ M. T. Burgy, G. R. Ringo, and D. J. Hughes, Phys. Rev. **84**, 1160 (1951).

¹² A. T. Stewart and G. L. Squires, Phys. Rev. **90**, 1125 (1953).

¹³ O. Halpern, Phys. Rev. **88**, 1003 (1952).

of scattering centers per unit volume with absorption and incoherent scattering cross sections σ_a and σ_i , respectively.

If absorption and incoherent scattering are neglected ($\gamma=0$), then total reflection occurs if a is positive and the angle ϕ is less than or equal to the critical angle

$$\phi_c = (4\pi Na)^{1/2}/k. \quad (2)$$

For positive a the primary effect of absorption and incoherent scattering is to round off the reflection coefficient at the critical angle. When a is negative there is no total reflection and absorption and incoherent scattering have almost no effect on reflection. Curves a, b, and c of Fig. 1 show, for monochromatic neutrons, typical reflection coefficients for positive a , $\gamma=0$; positive a , finite γ ; and negative a , respectively. Regardless of the sign of a , however, Eq. (1) approaches the value

$$r(k, a, \phi) \simeq \frac{1}{16} (4\pi Na / \phi^2 k^2)^2, \quad (3)$$

when $\phi \gg (4\pi N|a|)^{1/2}/k$.

Neutron scattering amplitudes generally lie between 2×10^{-13} and 10×10^{-13} cm. Therefore, only for angles less than about one degree and wavelengths greater than about 4 Å will there be any appreciable reflectivity. The very small angles involved imply zero-order Bragg reflection which is independent of molecular structure and molecular motion in the reflector. Hence there is no background from temperature diffuse scattering when neutrons are reflected by mirrors. Since the effect of absorption and incoherent scattering on the reflectivity is small, reflection methods are ideal for measuring the scattering amplitudes of highly absorbing materials where diffraction techniques are difficult to apply.¹⁴

The most direct, although not the most accurate, reflection method for determining a positive scattering amplitude is to measure the critical angle. There is seldom enough intensity to use Bragg diffracted monochromatic neutrons because of the long wavelength and precise collimation required,¹⁵ but it is still possible to observe the discontinuity in the slope at the critical angle using the spectrum transmitted through a polycrystalline filter.¹⁶ In this case the reflected intensity is given by

$$I(\phi) = \int_0^{k_f} r(k, a, \phi, \gamma) kn(k) dk, \quad (4)$$

where k_f is the cutoff wave number of the filter and $kn(k)$ represents the incident flux distribution. Introducing a spectrum with a sharp cutoff merely has the effect, shown in curves d and e of Fig. 1, of reducing the rate of decrease in reflected intensity above the critical angle.

¹⁴ Here a letter of M. Hamermesh [Phys. Rev. **77**, 140 (1950)] should be quoted, which discusses several applications of the measurement of coherent scattering to neutron phenomena.

¹⁵ E. Fermi and L. Marshall, Phys. Rev. **71**, 666 (1947).

¹⁶ D. J. Hughes and M. T. Burgoyne, Phys. Rev. **81**, 498 (1951); C. J. Heindl, I. W. Ruderman, J. M. Ostrowski, J. R. Ligenza, and D. M. Gardner, Rev. Sci. Instr. **27**, 620 (1956).

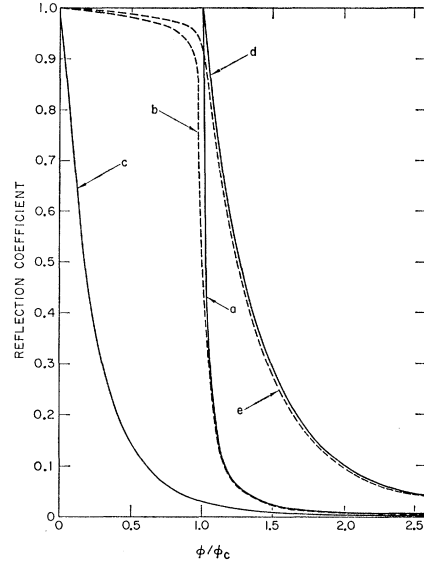


FIG. 1. Typical neutron reflection coefficients vs grazing angle ϕ in units of the critical angle $\phi_c = (4\pi N|a|)^{1/2}/k$. For monochromatic (4Å) neutrons: (a) positive scattering amplitude, no absorption or incoherent scattering, (b) positive scattering amplitude including absorption and/or incoherent scattering, (c) negative scattering amplitude. For Be-filtered neutrons (cutoff wavelength = 4Å): (d) same as (a), (e) same as (b).

Reflection methods are capable of greater accuracy when used to compare one scattering amplitude with another. Suppose we have two reflectors with positive scattering amplitudes a_1 and a_2 , respectively, and that for each reflector ϕ is larger than $(4\pi Na)^{1/2}/k$ for at least part of the incident spectrum. Neglecting the effects of incoherent scattering and absorption, if the incident angles are adjusted so that the same intensity is reflected from both reflectors, then their reflection coefficients [Eq. (1)] must be the same and

$$a_1/a_2 = (N_2/N_1)(\phi_1/\phi_2)^2. \quad (5)$$

This relation will also hold if both scattering amplitudes are negative, in which case there is no restriction on the size of ϕ .

The particular advantage of this method, which we will call the constant-intensity method, is that it is essentially independent of the incident neutron spectrum. The only way the spectrum influences the results is through the small differences in the reflection coefficients due to differences in incoherent scattering and absorption. There is also a small correction necessary for the effect of the finite angular resolution of the collimating system.

An alternative but less satisfactory approach, which we will call the constant-angle method, is to compare reflected intensities at the same angle. If $\phi \gg (4\pi N|a|)^{1/2}/k$ for all wavelengths in the incident spectrum, then from

Eq. (3) the reflected intensity is given closely by

$$I(\phi) = (\pi N a / \phi^2)^2 \int k^{-3} n(k) dk, \quad (6)$$

and the ratio of two scattering amplitudes will be

$$a_1/a_2 = (N_2/N_1)(I_1/I_2)^{1/2}. \quad (7)$$

Since $(I_1/I_2)^{1/2}$ can apparently be measured to greater accuracy than $(\phi_1/\phi_2)^2$, this method would seem preferable. However, the requirement on angle eliminates all total reflection and the reflected intensity will be very small and difficult to distinguish from the background. In practice, reasonable reflected intensities can only be obtained at angles small enough so that Eq. (7) is no longer valid. If the spectrum is known, the ratio a_1/a_2 can be determined by comparing intensities as calculated by integrating the reflection coefficients over the spectrum, but the possibility for systematic error is appreciably larger. If the scattering amplitudes are negative, the reflected intensity is much less affected by the long wavelength distribution and the constant-angle method is less spectrum-sensitive.

Mirror methods have certain unique advantages over other methods of measuring the n - p scattering amplitude. The very large incoherent scattering cross section of hydrogen, as well as temperature diffuse scattering, both of which interfere with diffraction measurements, have very little effect on mirror reflection. Also there are no large competing effects from other interactions such as was the problem with the parahydrogen cross-section measurements.

Liquid hydrocarbon mirrors provide a convenient means of comparing the n - p scattering amplitude with the accurately known carbon scattering amplitude. Since carbon has a positive nuclear scattering amplitude $(6.64 \pm 0.02) \times 10^{-13}$ cm,¹⁷ the scattering amplitude of a particular hydrocarbon can be either negative or positive depending on the ratio of hydrogen to carbon in the molecule. For a hydrocarbon, $N a = N_C a_C + N_H a_H$. Thus, if we have two mirrors made of liquid hydrocarbons with different hydrogen to carbon ratios, and if the incident angles are adjusted so that the liquids reflect with the same intensity, then

$$\frac{a_C}{|a_H|} = \frac{N_H^{(1)} - N_H^{(2)}(\phi_1/\phi_2)^2}{N_C^{(1)} - N_C^{(2)}(\phi_1/\phi_2)^2}, \quad (8)$$

provided both liquids have scattering amplitudes of the same sign.

¹⁷ *Neutron Cross Sections*, compiled by D. J. Hughes and R. Schwartz, Brookhaven National Laboratory Report BNL-325 (Superintendent of Documents, U. S. Government Printing Office, Washington, D. C., 1958), 2nd ed.; P. Egelstaff, J. Nuclear Energy 5, 203 (1957); J. R. Beyster, J. L. Wood, W. M. Lopez, and R. B. Walton, Nuclear Sci. and Eng. 9, 168 (1961).

III. EXPERIMENTAL APPARATUS¹⁸

The measurements were made with the apparatus shown schematically in Fig. 2. The neutron beam was defined by a 90-in. long collimator located in the reactor shield. Mounted between the interior and exterior collimator sections was a beryllium filter to scatter out fast neutrons. This filter was provided with liquid-nitrogen cooling and always kept cold while measurements were being made in order to get maximum beam intensity. The liquid mirror tray was in an airtight container mounted on a milling-machine table. Six BF₃ counters connected in parallel were used as the neutron detector. They were placed in a shielded box on a table which could be moved vertically. Thus both the mirror surface and the neutron detector could be precisely positioned with respect to the exterior collimator slit. A helium-filled plastic balloon was connected between the mirror tray and the detector to reduce air-scattering losses. For some of the measurements a slotted-cylinder neutron velocity selector was located between the mirror tray and the detector.

Collimation of the primary neutron beam presented a particular problem because of the small angles required and also because of the high fast-neutron flux from the Livermore pool-type reactor. The interior collimator section served only to provide some collimation of the neutrons entering the beryllium filter. Any fast neutrons leaking past or through the beryllium filter were stopped by a 6-in. steel block on which the exterior slit system was mounted. This block rested on a machinist's planar gauge and could be moved vertically to change the beam angle. The position of the exterior slits was determined by a dial indicator which measured the distance between the block and the base plate on which the planar gauge was mounted. The interior and exterior slits were 0.012 in. wide and were 44.6 in. apart so that the angular divergence of the beam was slightly less than ± 1 min. With this apparatus the minimum beam angle was 6 min and the maximum angle 36 min. Where necessary, interior surfaces of the collimator were cadmium-plated and then scored to reduce neutron reflections.

The stainless-steel box in which the mirror tray was located had 0.012-in. aluminum windows for the neutron beam at both ends and a micrometer depth gauge mounted on the top to determine the position of the liquid surface. Liquid temperatures were measured by means of a mercury thermometer submerged in the liquid and observed through a glass window on the top of the box. The mirror tray itself was 3 in. wide and 40 in. long and made of stainless steel. It was undercut at both ends to avoid concave menisci which might scatter neutrons from the beam at very small angles. Before measurements were made, the air was pumped

¹⁸ A more detailed description of the apparatus is given in W. C. Dickinson, L. Passell, W. Bartolini, and O. Halpern, Lawrence Radiation Laboratory Report UCRL-6320, 1961 (unpublished).

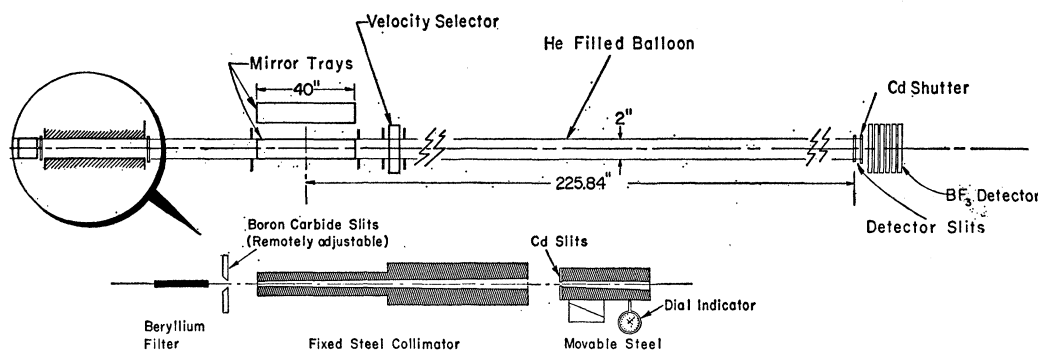


FIG. 2. Schematic plan view of neutron optics facility and enlarged side view (not to scale) of collimator.

out of the box and the liquid so that the only gas remaining was the vapor of the liquid.

The shielded box in which the BF₃ counters were mounted was made of steel in the shape of a cube 3 ft along a side and was filled with a mixture of boric oxide and paraffin. Neutrons reflected from the liquid mirror surface entered the box through a cadmium-lined channel. A pair of adjustable cadmium slits were mounted inside the box at the end of the channel immediately in front of the counters. The counters were filled to a pressure of 60 cm Hg with 96% enriched B¹⁰F₃ and were approximately 92% efficient for 4-A neutrons.

The intensity of the incident neutron beam was monitored by three BF₃ counters placed near the steel block on which the exterior collimator slits were mounted.

A mechanical neutron velocity selector¹⁹ was used to measure the incident neutron spectrum and also to remove long-wavelength neutrons from the reflected beam during the first measurements. Basically it consisted of a steel rotor 12.2 cm in radius and 10.7 cm long with 0.061-in. wide slots cut in the periphery parallel to the axis of rotation. The angle between the rotor axis and the neutron beam could be varied between zero and 6 deg. With the rotor axis parallel to the neutron beam the velocity selector acted as a high-pass filter transmitting only those neutrons with wavelengths greater than the cutoff wavelength

$$\lambda_c = h\psi / mL\omega,$$

where h is Planck's constant, ψ the angular slot opening, m the mass of the neutron, L the rotor length, and ω the rotor angular velocity. It was used in this way during the first measurements.

During the course of the first measurements it was discovered that the sensitivity of the BF₃ beam monitor counters depended to some extent on their previous history of exposure to neutrons. In order to avoid long-term inconsistencies in the data due to counter drifts,

a second tray was installed alongside the first (as shown in Fig. 2) and filled with dimethylnaphthalene (C₁₂H₁₂) which reflected the entire incident beam out to a grazing angle of 8.9 min. Thereafter, each reflected intensity was normalized to the intensity reflected from this standard liquid at an angle of 7.8 min.

All the hydrocarbons used were chosen because they are liquids with low vapor pressures and are available in highly purified form. Liquids with high vapor pressure were found to be unsatisfactory because the liquid level in the tray fell rapidly due to evaporation and also because the beam was scattered by the vapor above the liquid. We did not use any mixtures. While mixtures have the advantage of reducing the number of very pure liquids required they have several disadvantages. First, it is difficult to be certain of the exact proportions of the two liquids in the mixture, and second, there is some possibility that differences in the surface tensions of the two liquids might produce a difference in composition between the surface and the bulk liquid mixture.

The liquids were kept in stainless steel containers and, to avoid cross-contamination when the liquids were changed, the tray and associated piping were drained, flushed with acetone and ether, and then pumped dry before refilling.

IV. MEASUREMENTS

A. Angle

The angle ϕ was measured by essentially the same method as used by Burgy, Ringo, and Hughes.¹¹ First the mirror tray was lowered completely out of the incident beam and a profile of the thermal beam taken with narrow detector slits as is shown in the lower left-hand side of Fig. 3. The full width of this profile at the base is 0.188 in. compared to 0.182 in. expected from the slit geometry. After obtaining the direct beam profile, the mirror was raised until it intercepted the reflected beam, the detector slits were centered on it and opened until they accepted the entire beam. As the mirror moves vertically, the neutron beam traverses its surface until it overshoots one end or the other. Thus, by measuring the reflected thermal neutron intensity

¹⁹ M. Ruderman and W. C. Dickinson, Lawrence Radiation Laboratory Report UCRL-6319, 1961 (unpublished).

as the mirror and detector move up and down together, we obtained curves of the type shown in the upper part of Fig. 3. By setting the mirror halfway between the positions corresponding to half intensity, the beam axis was centered on the mirror tray. Then the position of the reflected beam was determined by taking its profile with narrow slits as shown in the lower right-hand side of Fig. 3. Finally, the angle was calculated from the distance between the centers of the direct and reflected beams and the distance between the counter slits and the center of the mirror tray.

Either dimethylnaphthalene or carbon tetrachloride was used as the reflecting liquid for the angle measurements because they both have large scattering amplitudes. Neutrons of 4-Å wavelength are totally reflected by these two liquids out to 8.9 and 13.3 min, respectively. Thus there was no possibility of distortion of the reflected beam which might affect the angle measurements.

The accuracy with which the angles were determined was limited primarily by the accuracy with which we could measure the distance between the direct and reflected beams. We estimated this to be between 0.004 and 0.005 in. Including the possibility of small errors in centering the beam on the mirror surface, we estimate that the uncertainty in the angle measurement was ± 0.05 min. This is also consistent with the standard deviation of the scatter in the angle measurements made at different times over a period of four weeks.

B. Spectrum

When the axis of the mechanical velocity selector is set at an angle with respect to the beam, it acts as a

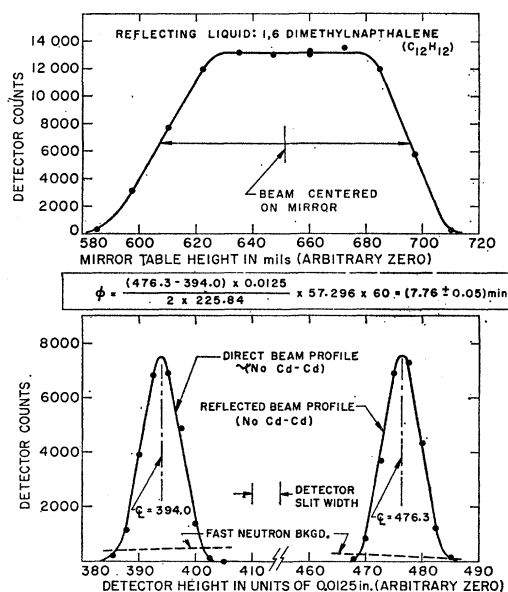


FIG. 3. Representative set of curves for the measurement of a reflection angle ϕ . Refer to text for explanation.

neutron monochromator. For the spectrum measurements we set the velocity selector at $\theta=4^\circ$ which gave us a fractional wavelength resolution $\Delta\lambda/\lambda_0$ of 0.207. The primary wavelength transmitted λ_0 , is determined by the angular velocity of the rotor ω , through the relation $\lambda_0 = h\theta/mR_0\omega$, where R_0 is the mean slot radius. We measured the beryllium-filtered thermal neutron intensity in the beam at 13 values of rotor angular velocity corresponding to neutron wavelengths from 6 to 17.6 Å, and then fitted the measurements to a function of the form $\phi(\lambda) = \text{const} \times \lambda^{-n(\lambda)}$ multiplied by an appropriate transmission function and integrated over the range of wavelengths transmitted by the velocity selector.¹⁹ The experimental data were fitted best when $n=0.03\lambda+5.7$, and this value was also assumed to be valid from 6 Å to the beryllium filter cutoff at 3.96 Å.

Our measurements showed the neutron flux decreased more rapidly at long wavelengths than a Maxwellian distribution for which the value of n would be 5. In fact, there are reasons for suspecting that the fall-off is even more rapid than our measurements indicated. First, there was the possibility that some long-wavelength neutrons were reflected from the slot walls rather than scattered or captured.²⁰ Second, we had no way of measuring the small background of neutrons with energies below the cadmium cutoff but above the beryllium filter cutoff. At the longest wavelengths the counting rates were so low that this background might have contributed an appreciable part of the observed counting rates.

C. Reflected Intensity

1. The Constant-Angle Measurements

Our first measurements were made at a fixed angle of 12.9 min with an angular spread of ± 2.3 min using a set of six liquid hydrocarbons: dimethylnaphthalene ($N_H/N_C=1.0$), *n*-butylbenzene ($N_H/N_C=1.4$), 4-vinylcyclohexene ($N_H/N_C=1.5$), *d*-limonene ($N_H/N_C=1.6$), tetradecylbenzene ($N_H/N_C=1.7$), and dodecene ($N_H/N_C=2.0$). Since the constant-angle method is sensitive to the spectral distribution of the incident neutrons, particularly the long-wavelength neutrons, the velocity selector was placed with its axis parallel to the beam so that the long-wavelength neutrons were not transmitted. Measurements were made with three different rotor velocities corresponding to long-wavelength cutoffs at 9.4, 12.0, and 14.1 Å. On the short-wavelength side the spectrum was cut off at 3.96 Å so that the measurements were actually made with a relatively small part of the incident neutron spectrum.

For each measurement the usual cadmium difference method was used to determine the fast neutron background. In addition we found a thermal neutron background which decreased rapidly as the angle increased, of the type described by Burgy, Ringo, and Hughes.

²⁰ L. Passell, W. C. Dickinson, and W. Bartolini, Rev. Sci. Instr. 32, 870 (1961).

The amount of this background in the reflected beam was determined by interpolating between the observed thermal neutron intensities on either side of the reflected beam. This procedure was also used for all subsequent measurements.

The thermal neutron background represented a significant fraction of the observed intensity for the liquids with low reflectivities and was a major source of systematic error. After careful investigation we discovered that the background came primarily from internal reflections within the collimator which was, at that time, a cadmium-plated slot 0.012 in. wide through the center of an 18-in. long steel block. The steel block was, therefore, removed and replaced by the collimation system described in Sec. III which reduced the thermal background to a small fraction of its previous value.

After modifying the collimation system to that described in Sec. III, the next measurement was a comparison of the neutron intensities reflected by water and dodecene ($N_H/N_C=2.0$) at 7.8 min. Since both liquids have negative scattering amplitudes, there was no total reflection, and the sensitivity of the measurement to the spectrum was not as great.²¹ Therefore, instead of using the neutron velocity selector to completely remove long-wavelength neutrons from the beam, we used a gold foil which selectively attenuated the long-wavelength neutrons. Hence we did two measurements: one with the entire beryllium-filtered spectrum and one with the 0.015-in. gold foil in the filtered beam. For these measurements and all the measurements that followed, reflected intensities were measured relative to the intensity reflected from dimethylnaphthalene as described in Sec. III.

2. The Constant-Intensity Measurements

The first of these measurements (our most accurate measurement, for reasons which will be discussed in Sec. V A) was made with four liquid hydrocarbons having positive-scattering amplitudes: *n*-butylbenzene ($N_H/N_C=1.4$), phenyl-*n*-hexane ($N_H/N_C=1.5$), *d*-limonene ($N_H/N_C=1.6$), and tetradecylbenzene ($N_H/N_C=1.7$). Reflected intensities were measured over angular intervals chosen so that each liquid reflected with about the same intensity. By using the constant-intensity method of analysis we eliminated the difficulties with the spectral distribution and therefore could use the entire beryllium-filtered spectrum. Two consecutive runs were made to check on the reproducibility of the data. Altogether they required about 100 hr. The beam, which had an angular divergence of slightly less than ± 1 min, was always kept centered on the mirror tray while data were taken by checking and adjusting the height of the liquid surface at approximately 20-min (time) intervals. The neutron detector slits were opened

to a width slightly greater than the width of the reflected beam and centered on it. Since many angles were used over an angular interval from 6 to 17 min, it was too time consuming to center the beam on the mirror and the detector on the beam each time by repeating the entire sequence of operations described above for the angle measurements. Instead we determined in a separate measurement the correct positions of the liquid surface and the detector box as a function of the position of the external collimator slit. Then, when the angle was changed, the vertical positions of the liquid surface and the detector were changed accordingly.

The second constant-intensity measurement was made with water and dodecene ($N_H/N_C=2.0$) over a range of angles from 6 to 11.5 min. Except for the fact that there was no total reflection, which reduced the reflected intensity considerably and required correspondingly longer counting times, this measurement was done in the same way as the previous measurement.

V. ANALYSIS OF DATA

Only one of the constant-intensity measurements yielded the desired accuracy, hence the data analysis for this measurement will be discussed in some detail.

A. Most Accurate Measurement

This is the first constant-intensity measurement described in Sec. IV C 2. Before Eq. (8) is applicable, several corrections must be made to the raw intensity data. Most of these corrections were small and tended to compensate one another to some extent so that the final corrected intensities almost always were within the statistical limits of uncertainty of the original observed intensities. These corrections, in approximate order of importance, are listed below.

(1) The reduction in reflected intensity due to incoherent scattering was calculated from Eq. (4) by use of an IBM 650. The results, seen in Fig. 4, show as would be expected that incoherent scattering has a

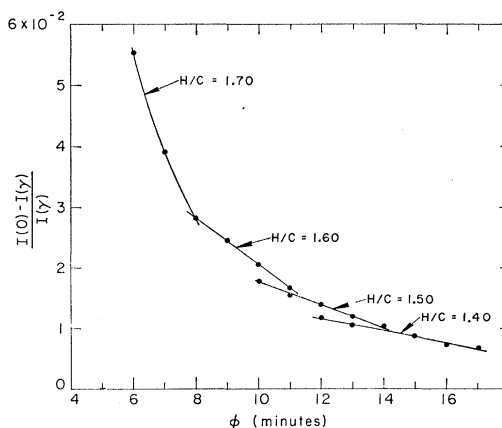


FIG. 4. Computed correction to measured intensity for incoherent scattering. (Most accurate measurement.)

²¹ To our knowledge, mirror measurements involving negative scattering amplitudes have not been reported in the literature previously.

TABLE I. Measured physical properties (at 25°C) of hydrocarbons used in most accurate measurement.

| Hydrocarbon | N_H/N_C | N_C (10^{+22} atoms/cc) | Density (g/cc) | Thermal exp coeff ($10^{-4}/^\circ\text{C}$) | Vapor pressure (mm Hg) |
|--|---------------------|---------------------------------|-------------------|--|------------------------------|
| n-butylbenzene ($\text{C}_{10}\text{H}_{14}$) | 1.4000 ± 0.0005 | 3.843 ± 0.002 | 0.85635 | 5.2 | 1.2 |
| phenyl-n-hexane ($\text{C}_{12}\text{H}_{18}$) | 1.497 ± 0.001 | 3.735 ± 0.002 | 0.85586 | 9.0 | 0.10 |
| d-limonene ($\text{C}_{10}\text{H}_{16}$) | 1.600 ± 0.001 | 3.710 ± 0.002 | 0.8388 | 7.4 | 2.1 |
| tetradecylbenzene ($\text{C}_{20}\text{H}_{34}$) | 1.702 ± 0.006 | 3.734 ± 0.002 | 0.85084 | 7.9 | 0.5 |

greater effect on the reflectivity as the hydrogen concentration increases and as the angle decreases. All measured intensities were increased to the values that would be expected in the absence of incoherent scattering.

(2) The fractional correction to the observed intensity due to the finite angular resolution of the collimating system is given by

$$\delta(\phi_0) = \frac{\int_{\phi_0-\Delta\phi}^{\phi_0+\Delta\phi} I(\phi)T(\phi)d\phi - I(\phi_0)\Delta\phi}{\int_{\phi_0-\Delta\phi}^{\phi_0+\Delta\phi} I(\phi)T(\phi)d\phi}, \quad (9)$$

where the transmission $T(\phi)$ for the collimating system is

$$T(\phi) = (1/\Delta\phi)[\phi - (\phi_0 - \Delta\phi)] \text{ for } (\phi_0 - \Delta\phi) \leq \phi \leq \phi_0 \\ = (1/\Delta\phi)[(\phi_0 + \Delta\phi) - \phi] \text{ for } \phi_0 \leq \phi \leq (\phi_0 + \Delta\phi).$$

If we assume that $I(\phi) = \text{const} \times \phi^{-x}$, then it can be shown to first order that

$$\delta(\phi_0) \simeq [x(x+1)/12](\Delta\phi/\phi_0)^2, \quad (10)$$

and since $\Delta\phi$ is fixed by the dimensions of the collimator, $\delta(\phi_0)$ will decrease as the angle ϕ_0 increases. In the region where the data were taken, the intensity varied

nearly as the inverse fifth power of the angle and $\delta(\phi_0)$ could be computed with sufficient accuracy by assuming $x=5$. As a cross-check, $\delta(\phi_0)$ was also determined by using for $I(\phi)$ the values computed from Eq. (4). The results are shown in Fig. 5 together with the plot of Eq. (10) for $x=5$. It is an interesting coincidence that the angular resolution of our collimator was such that this correction almost exactly canceled the incoherent scattering correction.

(3) The thermal background decreased as the angle increased, i.e., as the reflected beam moved away from the mirror tray. It never exceeded 5% of the reflected intensity and was usually much smaller. Because of the low intensity of this background it was impossible to determine how it varied through the region of the reflected beam, although it was slightly larger on the small-angle side. The observed intensity was corrected for this background by simply subtracting the average of the measured thermal counts on either side of the reflected beam.

(4) The liquid temperatures varied over a range of about 2°C during the data runs. If α is the volume expansion coefficient, then the fractional change in intensity for a change ΔT in temperature is given by $\Delta I/I = -2\alpha\Delta T$. Expansion coefficients for the hydrocarbons used were all between 5 and 9×10^{-4} per °C (see Table I), hence the corrections were of the order of a few tenths of 1%.

(5) Air and vapor above the liquid reduce the reflected intensity by absorbing and scattering the beam. Although the air in the mirror box was pumped off initially, there were still hydrocarbon vapor and small amounts of air which leaked back into the box because it was not completely tight. All the hydrocarbons used had vapor pressures smaller than 2.5 mm Hg (Table I) at room temperature so the losses in intensity due to scattering in the 100-cm length of the mirror were of the order of 1% or less. The scattering of the air which leaked into the box was generally slightly larger than this.

(6) There was a correction for a 2% decrease in the intensity of the incident beam as the angle was increased from 8 to 18 min. This was inherent in the apparatus. Since the reflected intensity from the standard liquid was always measured at the same angle, all other reflected intensities were normalized to the incident intensity at this angle.

Figure 6 is a graph of corrected measured intensity

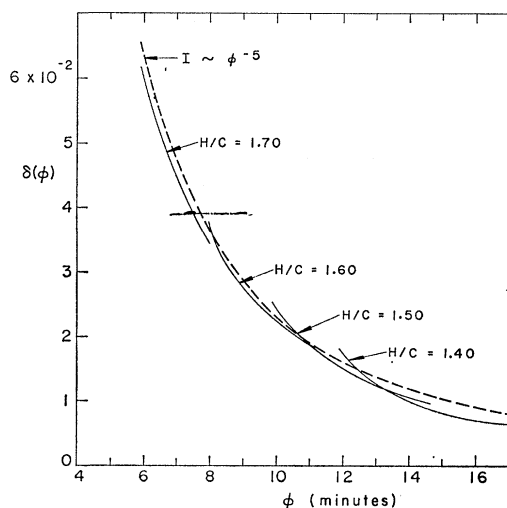


FIG. 5. Computed correction to measured intensity for finite-angular resolution. (Most accurate measurement.)

versus angle for each of the four liquids. The circles represent the data points obtained in the first run; the squares are those obtained in the second run.

It should be noted that $a_C/|a_H|$ is rather insensitive to nonindependent changes in intensity. Assume that the reflected intensity from each of two hydrocarbons

$$\frac{\Delta(a_C/|a_H|)}{a_C/|a_H|} \sim \frac{2[(N_H^{(1)}/N_C^{(1)}) - (N_H^{(2)}/N_C^{(2)})](\phi_1/\phi_2)^2}{5[(N_H^{(1)}/N_C^{(1)}) - (N_H^{(2)}/N_C^{(2)})](\phi_1/\phi_2)^2[1 - (\phi_1/\phi_2)^2]} \left(\frac{\Delta I_1}{I_1} - \frac{\Delta I_2}{I_2} \right). \quad (11)$$

Clearly, if the intensities for two liquids are in error by the same percentage it will have no effect on the value of $a_C/|a_H|$. As a typical example, for the 1.5 and 1.6 liquids at angles 12.0 and 9.55 min, respectively, Eq. (11) yields

$$\frac{\Delta(a_C/|a_H|)}{a_C/|a_H|} \sim 0.1 \left(\frac{\Delta I_1}{I_1} - \frac{\Delta I_2}{I_2} \right),$$

and for an accuracy of 0.3% in $a_C/|a_H|$ we require only that $(\Delta I_1/I_1) - (\Delta I_2/I_2)$ be less than 3%. Since the reflected intensities from all the liquids are affected in the same way, although not necessarily to the same extent, by most important sources of error discussed above, it is apparent that their effect on $a_C/|a_H|$ will be small. This is a particular advantage of the comparison method.

Uncertainties in chemical composition of the hydrocarbons have a more direct effect on $a_C/|a_H|$ since we can expect no correlation in the errors. Assuming again that all the N_C 's are about the same and that the uncertainties in the composition of the hydrocarbons are all roughly comparable, we obtain

$$\frac{\Delta(a_C/|a_H|)}{a_C/|a_H|} \sim \frac{(\phi_2^4 + \phi_1^4)^{1/2} (N_H/N_C)}{\phi_2^2 (N_H^{(1)}/N_C^{(1)}) - \phi_1^2 (N_H^{(2)}/N_C^{(2)})} \frac{\Delta(N_H/N_C)}{N_H/N_C}.$$

Again using the 1.5 and 1.6 liquids as an example, we have

$$\frac{\Delta(a_C/|a_H|)}{a_C/|a_H|} \sim 3 \frac{\Delta(N_H/N_C)}{N_H/N_C},$$

and it follows that 0.3% accuracy in $a_C/|a_H|$ will require 0.1% accuracy in N_H/N_C .

After obtaining the purest liquids available, precise chromatographic analyses were made, both before and after the measurement, to determine what impurities were present and in what concentrations. The resulting values of N_H/N_C and the measured densities are listed in Table I.

Since the angles corresponding to a given reflected intensity must be found in order to determine $a_C/|a_H|$, it was necessary to interpolate between the corrected measured intensities. The reflected intensity data for

is changed in the same way but not to the same extent by some common cause. Since I varies approximately as ϕ^{-5} , the fractional error in ϕ due to the error in I would be $\frac{1}{5} \Delta I/I$. From an analysis based on Eq. (8), assuming each liquid has about the same N_C , we obtain as the resultant fractional error in $a_C/|a_H|$:

each hydrocarbon was therefore least-squares fitted to a curve computed using Eq. (4). It was necessary to adjust the measured neutron spectrum empirically in order to obtain a satisfactory fit. Reasons were given above why the measured spectrum might be in error at the long wavelengths, but in any event the calculated curves, shown in Fig. 6, are more accurate smoothing functions than completely empirical smooth curves drawn through the experimental points. Since the calculated curves serve only to improve the interpolation of intensities, the error introduced in the final result by an error in the spectrum should be small.

We chose seven intensities, shown by horizontal dotted lines in Fig. 6, as close to the measured intensities as possible and found the corresponding angles from the fitted curves. Values of $a_C/|a_H|$ were calculated from Eq. (8) for each pair of hydrocarbons at each of the seven intensities. The weighted averages are given in Table II. The weighted average of these six values is 1.772 ± 0.002 where the quoted uncertainty is the

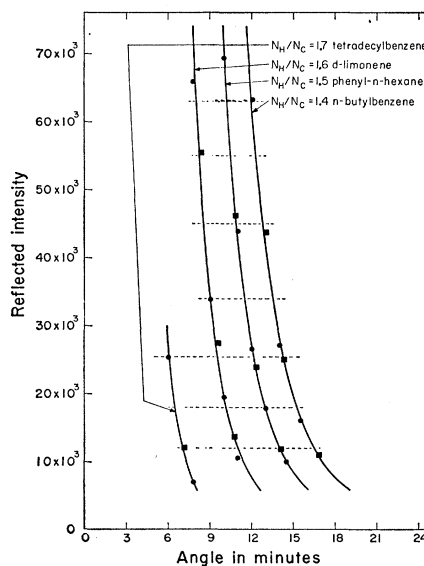


FIG. 6. Corrected experimental intensity data and machine-calculated curves for most accurate measurement. The dashed lines correspond to the intensities chosen for data analysis. The circles represent data points obtained in the first run; the squares are those obtained in the second run three days later. The ordinate corresponds to the number of detector counts for a fixed number of counts from the standard reflecting liquid.

TABLE II. Weighted average values of $a_C/|a_H|$ obtained in most accurate measurement.

| N_H/N_C of liquid hydrocarbon pairs | $a_C/ a_H $ |
|---------------------------------------|-------------------|
| 1.4 and 1.5 | 1.779 ± 0.005 |
| 1.4 and 1.6 | 1.772 ± 0.002 |
| 1.4 and 1.7 | 1.772 ± 0.006 |
| 1.5 and 1.6 | 1.769 ± 0.008 |
| 1.5 and 1.7 | 1.771 ± 0.006 |
| 1.6 and 1.7 | 1.772 ± 0.008 |

standard deviation due to the combined effects of the uncertainties in the measured angles, the measured hydrogen-to-carbon ratios and the measured densities.

To check for the possibility of some long-term effect on accuracy, the first and second data runs were also analyzed separately. The weighted averages were found to be 1.768 and 1.778, respectively. The weighted average of these two values was determined to be 1.772 as expected.

The systematic error associated with the fitting of the data was estimated by taking the smoothing functions calculated with the measured spectrum and adjusting them empirically to give the best fit. A re-analysis of the data then gave $a_C/|a_H| = 1.771$. We hence estimate the systematic error due to this cause to be no greater than ± 0.002 .

A small contribution from the neutron-electron coherent scattering amplitude must be taken into account in order to obtain the ratio of the nuclear scattering amplitudes which may be written as

$$\frac{a_C}{|a_H|}(\text{nuclear}) = \frac{a_C}{|a_H|} \left(1 + \frac{a_e}{a_H} \right) + 6 \frac{a_e}{a_H}.$$

Since the neutron-electron amplitude a_e is -1.4×10^{-16} cm,²² the final ratio of the nuclear amplitudes is found to be²³ from this measurement

$$a_C/|a_H|(\text{nuclear}) = 1.775 \pm 0.004.$$

B. Other Measurements

The second constant-intensity measurement was a comparison of the reflected intensity from dodecene ($N_H/N_C = 2.0$) and water. Incoherent scattering did not influence the reflectivity appreciably, because the scattering amplitudes of both liquids are negative. The effect of finite-angular resolution was also small because the intensity did not change as rapidly with angle. Corrections for the other effects were of about the same magnitude as before. Figure 7 shows the corrected data

points and the fitted curves computed from Eq. (4). Three intensities were chosen as close to the measured intensities as possible and the corresponding angles found from the fitted curves. For this measurement, Eq. (8) is replaced by

$$\frac{a_C}{|a_H|} = \frac{N_H^{(1)} - N_H^{(2)}(\phi_1/\phi_2)^2}{N_C^{(1)} - N_C^{(2)}(a_O/a_C)(\phi_1/\phi_2)^2}.$$

Assuming $a_O/a_C = 0.878 \pm 0.004$ we obtain, from this measurement, $a_C/|a_H| = 1.781 \pm 0.010$.

The two constant-angle measurements are described in Sec. IV C 1. The first measurement was made at a fixed angle of 12.9° min with a set of six hydrocarbons with hydrogen-to-carbon ratios of 1.0, 1.4, 1.5, 1.6, 1.7, and 2.0. In addition to subtracting off fast and thermal background, corrections were made for neutron monitor and detector drift, variations in the temperature of liquids, and scattering of the neutron beam by the vapor above the liquid. Of these corrections the thermal background and monitor drift were the most important.

The data analysis consisted of numerically integrating Eq. (4) with an IBM 650 computer, assuming various values of $a_C/|a_H|$ and determining the value that gave the best least-squares fit to the experimental points. The spectral distribution used in the integration was obtained by calculating the transmission (as a function of neutron wavelength) of the neutron velocity selector with its axis of rotation parallel to the neutron beam and rotating at 8, $9\frac{1}{2}$, and 11 rps and then weighting the measured incident spectrum accordingly. Figure 8 shows the data plotted as $I^{1/2}/N_C$ versus the hydrogen-to-carbon ratio of the liquids. The data obtained at the three angular velocities were best fitted by values of

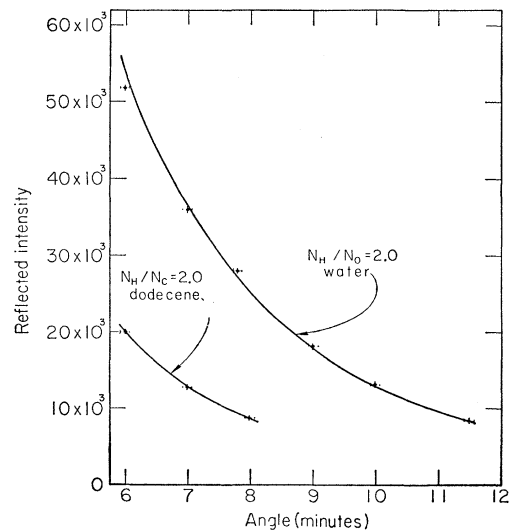


FIG. 7. Corrected experimental data and machine-calculated curves for the second constant intensity measurement. The ordinate corresponds to the number of detector counts for a fixed number of counts from the standard reflecting liquid.

²² D. J. Hughes, J. A. Harvey, M. D. Goldberg, and M. J. Stafne, Phys. Rev. **90**, 497 (1953).

²³ There is 0.0156% deuterium present in normal hydrogen. The neutron-proton scattering amplitude is 0.028% larger in magnitude than the neutron-(proton+0.016% deuterium) amplitude. This is not quite large enough to affect the last significant figure in our measured value of $a_C/|a_H|$.

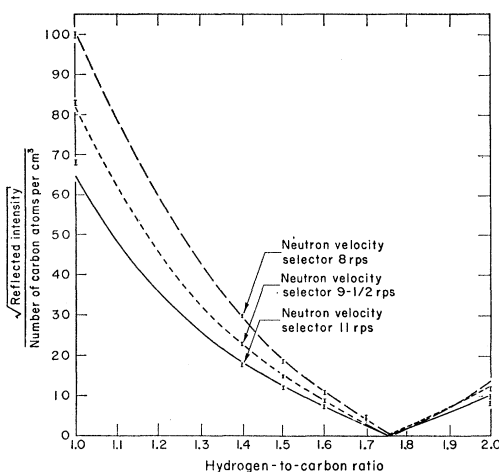


FIG. 8. Corrected experimental data and machine-calculated curves for the first constant-angle measurement. Ordinate in arbitrary units.

$a_C/|a_H| = 1.754, 1.750,$ and 1.765 , respectively. The curves fitted to the experimental data of Fig. 8 were calculated using these values. Note that they are not straight lines as would be expected if the conditions of Eq. (7) were satisfied.

Making reasonable assumptions as to the limits of error introduced by the uncertainty in the thermal background and the spectrum, we obtain from this measurement $a_C/|a_H| = 1.756 \pm 0.015$.

The second constant-angle measurement was a comparison of the intensities reflected by water and dodecene at a fixed angle of 7.8° . Since both liquids have negative-scattering amplitudes, the reflected intensity would be expected to be less sensitive to the incident spectrum. We tested this experimentally by making measurements with the beryllium-filtered spectrum both with and without a 0.015-in. thick gold foil in the incident beam. This foil attenuates 12-A neutrons about three times more than it attenuates 4-A neutrons.

Again it was only possible to analyze the results by integrating Eq. (4) numerically. Using 0.878 for the oxygen-to-carbon scattering amplitude, we found that the calculated intensity ratios agreed with the observed ratios when we assumed $a_C/|a_H| = 1.768 \pm 0.018$ for both the no-gold-foil and the 0.015-in. gold-foil data.

In each of the three measurements discussed in this section, sources of systematic error were of considerably greater importance than the usual statistical error contributions. Hence the uncertainties quoted in the $a_C/|a_H|$ values for these three measurements are attempted estimates of limits of error. The weighted average of these three measurements is $a_C/|a_H| = 1.773 \pm 0.008$, and after correcting for the contribution from neutron-electron scattering we obtain 1.776 ± 0.008 (limit of error), in excellent agreement with the value quoted above from our most accurate measurement.

We wish to emphasize that the constant angle meas-

urements are of only qualitative significance. They are described here for completeness and to indicate the difficulty of eliminating sources of systematic error in such measurements.

VI. CONCLUSIONS

The presently accepted value for the bound-atom coherent scattering cross section of carbon is $5.50 \pm 0.04 \text{ b}$ ¹⁷ based on the work of Koehler and Wollan. There is also an unpublished result of $5.53 \pm 0.03 \text{ b}$ obtained by Sailor.¹⁷ We will take as the present best value $5.52 \pm 0.03 \text{ b}$. The bound-atom coherent scattering amplitude $a_C = (\sigma_C/4\pi)^{1/2}$ is therefore $(6.63 \pm 0.02) \times 10^{-13} \text{ cm}$. On correcting for the neutron-electron scattering amplitude, the nuclear coherent scattering amplitude of carbon is $(6.64 \pm 0.02) \times 10^{-13} \text{ cm}$. Combining this value with the result of the present measurement, $a_C/|a_H| = 1.775 \pm 0.004$, gives for the bound nuclear scattering amplitude of hydrogen $a_H = (-3.74 \pm 0.02) \times 10^{-13} \text{ cm}$. (The bound-atom value for hydrogen is the same because the correction for the neutron-electron amplitude is much smaller than the present uncertainty.)

If we combine this value of the hydrogen scattering amplitude with the measurement of the neutron-proton scattering cross section,²⁴ we have two equations relating the free-atom triplet and singlet-scattering amplitudes:

$$\begin{aligned} \frac{3}{4}a_t^2 + \frac{1}{4}(4\pi a_s^2) &= \sigma_H = (20.36 \pm 0.10) \times 10^{-24} \text{ cm}^2, \\ \frac{3}{4}a_t + \frac{1}{4}a_s &= a_H(\text{free atom}) \\ &= \frac{1}{2}(-3.74 \pm 0.02) \times 10^{-13} \text{ cm}. \end{aligned}$$

Solving these equations we find

$$\begin{aligned} a_t &= (5.40 \pm 0.02) \times 10^{-13} \text{ cm}, \\ a_s &= (-23.67 \pm 0.06) \times 10^{-13} \text{ cm}. \end{aligned}$$

In the effective range theory the radius of the deuteron R is related to the effective range of the triplet interaction r_t at zero energy by the equation²⁵

$$1/R = [(1/a_t) + (r_t/2R^2)],$$

where the size of the deuteron is defined in terms of the reduced mass μ , and the binding energy E_B , by the relation $R = (\hbar^2/2\mu E_B)^{1/2}$. Using as the presently accepted best value of the deuteron binding energy $2.225 \pm 0.003 \text{ Mev}$ ²⁶ and the value for the triplet scattering amplitude given above, we find

$$r_t = (1.74 \pm 0.03) \times 10^{-13} \text{ cm}.$$

This result is in excellent agreement with the value $r_t = (1.74 \pm 0.03) \times 10^{-13} \text{ cm}$ derived from the measured cross section for photodisintegration of the deuteron.²⁷

²⁴ E. Melkonian, Phys. Rev. **76**, 1744 (1949).

²⁵ J. M. Blatt and V. F. Weisskopf, *Theoretical Nuclear Physics* (John Wiley & Sons, Inc., New York, 1952).

²⁶ E. L. Chupp, R. W. Jewell, and W. John, Phys. Rev. **121**, 234 (1961).

²⁷ R. E. Wilson (private communication).

At present, the accuracy with which the singlet and triplet-scattering amplitudes are known is more limited by the accuracy of the zero-energy (n,p) cross section than by the accuracy of the (n,p) scattering amplitude.

ACKNOWLEDGMENTS

We would like to express our appreciation for the technical assistance of E. R. Hanson, W. F. Beisley, and

M. G. Shoemaker. We wish to thank V. L. DuVal for his careful measurements of the purities and physical properties of the hydrocarbons and E. M. Vienop for her assistance in the IBM 650 calculations. Special thanks are due W. Bartolini for assistance in taking and analyzing data. Finally we wish to express our thanks to Dr. A. J. Kirschbaum for his continued encouragement and support of this research.

Decay Studies of the Even-Even Isotopes, Er^{172} and $\text{Dy}^{166}\dagger$

RAY GUNNINK AND A. W. STONER

Industrial Reactor Laboratories, Incorporated, U. S. Rubber Company, Plainsboro, New Jersey

(Received November 10, 1961)

Er^{172} and Dy^{166} , with half-lives of 48.7 ± 0.5 hr and 81.8 ± 0.2 hr, respectively, were produced by double neutron capture from Er^{170} and Dy^{164} . Gamma rays of the following energies were found in the decay of Er^{172} : two coincident 50-kev radiations, 72, 128, 170, 200, 410, 440, and 610 kev. The proposed energy levels for Tm^{172} consistent with the data are as follows: 410, 440, 482, 538, and 610 kev. $\log ft$ values of beta transitions indicate that the 538- and 610-kev levels have spin assignments of 0 or 1 with positive parity. The following gamma transitions were found in the decay of Dy^{166} : 84, 291, 343, 373, and 427 kev. In addition to showing conversion electrons of the 84-kev transition, permanent-magnet spectrometer studies revealed the presence of two additional transitions of 30 and 54 kev which were not observed in scintillation studies. The multipolarity of the low-energy transitions are as follows: 30 kev- $M1$, 54 kev- $E2$, and 84 kev- $M1$. The proposed energy levels for Ho^{166} are at 54, 84, 375, and 427 kev.

INTRODUCTION

THE species Dy^{166} and Er^{172} are of special interest because they are among the few examples of the decay of an even-even nuclide to the excited levels of an odd-odd nuclide in the region of high-nuclear deformation. Ketelle¹ and Butement,² first reported a new 81-hr activity from the high-flux neutron irradiation of dysprosium. Nethaway *et al.*³ similarly reported a new 49-hr activity from erbium irradiations. These activities were demonstrated to be Dy^{166} and Er^{172} by genetic relationships. More recently the results of experiments carried out concurrently with these have been reported for both of these isotopes.⁴⁻⁷

Source Production and Purification

Erbium oxide enriched to 87.3% in Er^{170} was used to produce Er^{172} activity by double neutron capture. The

interfering activities also produced were Er^{169} , Er^{171} , Tm^{172} and small amounts of activated contaminants. Tm^{172} and the contaminants were removed using ion-exchange column separation techniques. The 7.5-hr Er^{171} activity, was allowed to decay away before subsequent investigations were begun. Er^{169} is essentially a pure beta emitter except for an 8-kev converted transition, bremsstrahlung and possibly a small percentage of other low-energy radiations. To produce Dy^{166} activity, natural abundance dysprosium was irradiated. The only major contaminant, Ho^{166} , was removed by ion exchange.

The neutron irradiations were carried out in the 5-megawatt reactor of Industrial Reactor Laboratories, Inc., Plainsboro, New Jersey. An "in-core" irradiation facility which has a thermal neutron flux $> 1 \times 10^{14} n/cm^2 \text{ sec}$ was frequently used. The length of the irradiations was about 90 hr.

Experimental Equipment

A 3×3 -in. well-type, and a 3×3 -in. solid NaI(Tl) crystal, housed in a specially lined lead cave similar to that described by Heath,⁸ were used to study the gamma emissions of the isotopes. The 3×3 -in. well-type crystal was calibrated for photopeak counting efficiency⁹

[†] This work was supported by the U. S. Air Force Office of Scientific Research.

¹ B. H. Ketelle, Phys. Rev. **76**, 1256 (1949).

² F. D. S. Butement, Proc. Phys. Soc. (London) **A63**, 532 (1950).

³ D. R. Nethaway, M. C. Michel, and W. F. Nervik, Phys. Rev. **103**, 147 (1956).

⁴ R. G. Helmer and S. B. Burson, Bull. Am. Phys. Soc. **6**, 72 (1961); Argonne National Laboratory Report ANL-6270, 1961 (unpublished), and Phys. Rev. **123**, 992 (1961).

⁵ R. G. Helmer, S. B. Burson, Bull. Am. Phys. Soc. **4**, 427 (1959) and Phys. Rev. **119**, 788 (1960).

⁶ J. S. Geiger, R. L. Graham, and G. T. Ewan, Bull. Am. Phys. Soc. **5**, 255 (1960).

⁷ C. J. Orth and B. J. Dropesky, Phys. Rev. **122**, 1295 (1961).

⁸ R. L. Heath, Atomic Energy Commission Report IDO-16408, 1957 (unpublished).

⁹ Ray Gunnink and A. W. Stoner, Anal. Chem. **33**, 1311 (1961).